BOLETIN DE LA SOCIEDAD ESPAÑOLA DE
Cerámica y Vidrio
A R T I C U L O

Near-field optical and atomic force microscopy studies on $RbTiOPO_4$ single crystal with ferroelectric domains

J. CANET-FERRER, L. MARTÍN-CARRÓN, J. L. VALDÉS, J. MARTÍNEZ-PASTOR.
Instituto de Ciencia de los Materiales de la Universidad de Valencia, E-46071 Valencia, Spain.
J. J. Carvajal and F. Diaz
Laboratori de Física i Cristalografía de Materials, Universitat Rovira i Virgili, E-43005 Tarragona, Spain.

We have developed a Scanning Near-Field Optic Microscope (SNOM), which is based on a commercial tuning-fork sensor, capable of measuring the topography and the optical signal, at the same time. We have measured the SNOM transmission, as well as the topography, of an $RbTiOPO_4$ single crystal, which exhibits two kinds of macroscopic ferroelectric domains. A chemical selective attack has been performed to distinguish them. As a consequence, we obtained zones with a noticeable roughness (C^-) in comparison with the flat aspect of the other ones (C^+). The SNOM topography images have been compared to Atomic Force Microscopy ones, which has a better resolution. The changes observed in the transmission measurements are due to different effects: i) variations of the dielectric constant at the interface walls between domains; ii) light scattering, wavelength dependent, at the grains in the C^- face. Finally, we have determined the angles formed at the domain-walls between inverted domains, which are measured to be higher than 90º and close to 135º, as could be expected, because of the combination between [1 1 0], [-1 1 0], [1 0 0] and [0 1 0] directions of the orthorhombic lattice.

Keywords: Ferroelectric, Domains, $RbTiOPO_4$, Near-field, AFM

Estudios de microscopía óptica de campo cercano y de fuerza atómica en $RbTiOPO_4$ monocristalino con dominios ferroeléctricos

Hemos desarrollado un Microscopio Óptico de Campo Cercano (SNOM) que es capaz de adquirir una señal óptica, al mismo tiempo que la topografía, basado en un sensor de fuerza lateral comercial. Con este microscopio hemos medido la transmisión óptica en campo cercano, así como la topografía, de un cristal de $RbTiOPO_4$, que exhibe dos tipos de dominios ferroeléctricos macroscópicos. Previamente, la muestra había sido sometida a un ataque químico selectivo, con el que se pueden distinguir dos zonas diferentes, una con una rugosidad apreciable (C^-) y otra con aspecto perfectamente plano (C^+), aspecto que tenía la superficie antes del ataque. Hemos comparado las imágenes de topografía del SNOM con otras tomadas usando un Microscopio de Fuerzas Atómicas, con mayor resolución espacial. Los cambios observados en las medidas de transmisión son debidos a dos tipos de efectos: i) las variaciones en la constante dieléctrica en las paredes de dominios y sus cercanías; ii) la dispersión de luz, dependiente de la longitud de onda, en los granos de la cara C^-. Por último, hemos determinado los ángulos que forman las paredes de dominios invertidos, que resultan ser mayores de 90º y bastante cercanos a 135º, en promedio, tal y como se podría esperar, debido a la combinación de las direcciones [1 1 0], [-1 1 0], [1 0 0] y [0 1 0] de la estructura ortorrómbica.

Palabras clave:ferroeléctrico, dominios, $RbTiOPO_4$, SNOM y AFM

1. INTRODUCTION

Almost fifty years ago, the possibility of developing Scanning Probe Microscopies was predicted (1). Such new microscopic techniques were based on electrostatic interactions, at nanomethre scale, and their resolution was expected to be greater than that of the optical microscope, which was limited by the light diffraction limit. These techniques have been satisfactory developed, with nanometric resolution, since 1987 (2, 3). A new research line has also been opened given that some of them are able to obtain electro-optical and mechanical properties simultaneously, together with enlarged images of a vast kind of samples. Therefore, they could be useful to measure physical properties at different nano and micrometric areas, and to observe the physical effects in thin films, produced by the confinement, and compare them with those in bulk materials (4-6)

The Scanning Near-Field Optical microscope (SNOM) is one of these novel techniques, which, with a resolution better than 100 nm, allows imaging the near-field features of the sample surface under study (1, 7). We have developed a SNOM based on a commercial tuning-fork sensor head and an optical fiber tip attached to one side of this sensor. The resolution of this scanning microscope depends on the fiber-optic aperture and it provides the possibility to record simultaneously the SNOM optical images (transmission or reflectivity), as well as the topography of the scanned area in the sample.

$RbTiOPO_4$ (RTP), which is isostructural with $KTiOPO_4$ (KTP), is a ferroelectric material at room temperature with orthorhombic structure. Above the critical temperature, the structure is cubic and the material becomes paraelectric (8-10). The lock of inversion symmetry in the orthombic structure of the ferroelectric phase is the main reason for which these compounds show interesting non-linear optical (NLO) properties (11). Doping with lanthanide, the photoluminescence of the ion and the NLO properties of

the material can be merged (12). Apart from the interest in the NLO properties, these materials (and other ferroelectric materials as, for example, $LiNbO_3$, $KNbO_3$, etc.) have attracted much attention, because one can obtain domains in a periodic way intentionally ($LiNbO_3$) or even unintentionally ($KNbO_3$), which is the basis for applications in quasi-phase matched nonlinear optics and acoustics [13, 14].

Several studies about the structure and ferroelectric domain inversion in KTP (or RTP) by X-ray Diffraction and Scanning Electron Microscopy can be found in literature (15, 16). We have studied the Atomic Force Microscopy (AFM) and SNOM topography, as well as the near field optical transmission (at nano- and micro-metric scale) of a $RbTiOPO_4:Er^{3+}$ single crystal sample (the Er^{3+} doping was less than 0.2% and it did not have any influence on the results presented in this work). First, a chemical selective attack has been performed to distinguish between these domains, and the topography has been characterized with a roughness analysis by AFM. In the next step, the domain walls have been observed by AFM and SNOM, in the latter case obtaining both topographic and optical information. The angles defined at the C^+-C^- domain wall have been measured in many topography/optical images of our microscope. The most probable angle is in good agreement with the crystallographic predictions. Finally, we point out the importance of this emerging technique to characterize the domain walls at the nanometer scale, without the need of etching and, therefore, without damaging the sample.

2. EXPERIMENTAL DETAILS

The structure of KTP family has been studied by Thomas et al. (9). RTP is isomorphic with KTP witle orthorhombic structure $Pna2_1$ at room temperature and lattice parameters a = 12.974 Å, b = 6.494 Å and c = 10.564 Å. The sample studied has been obtained by top-seeded-solution growth (TSSG). Two C-oriented RTP:Er^{3+} seeds were placed close to the furnace of a solution with the appropriate amounts of Rb_2CO_3, $NH_4H_2PO_4$, TiO_2 and Er_2O_3 (17). This method, in combination with a slow-cooling process, was used to obtain crystals suitable for optical investigation. A selective chemical attack was performed after polishing the sample, in order to distinguish between the two macroscopic domains. As a result, the C^- domain is damaged, presenting a rough surface, while the C^+ domain maintains the same flat aspect than before the etching process (15, 16).

We have obtained the high-resolution topography of the sample with a commercial AFM (Nanotec Electrónica), based on a standard head for Scanning Force Microscopy and a patented piezoelectric scanner (17.5x17.5x3 μm^3), which supports the sample holder. The AFM tip (PointProbePlus from Nanosensors) has an elastic constant k=40N/m, a tip radius of 10 nm and a resonance frequency around 150 kHz. The images were acquired under non-contact tapping mode and used to compare with the topography obtained with our SNOM, which has the possibility to move in the xy-plane with a precision better than 100 nm (inertial stepper motors from Attocube Systems AG). The SNOM is based on a commercial tuning-fork quartz sensor (Attocube Systems AG), which has been conveniently connected by us to a commercial AFM-electronics (Nanotec Electrónica), as also the optical signal and piezoelectric ceramics for x-y scan and z-axis motion. The probe is a metal coated monomode optical fibre tip fabricated by us (FH wetting etching and aluminium coating by thermal evaporation). The shear-force resonance of the tuning-fork changes from 32.7 to 33.5 kHz, approximately, after gluing the fibre tip, at the same time that the Q factor reduces from 3000 to 500, typically. The sample surface was illuminated with light of several wavelengths (660 nm, 785 nm and 980 nm) using different laser diodes biased with a precision laser diode controller (Thorlabs). The transmission images, as well as the topography ones, were all recorded for these different wavelengths. The transmitted light was collected with a germanium detector. A simplified scheme of the SNOM basics is depicted in Fig. 1

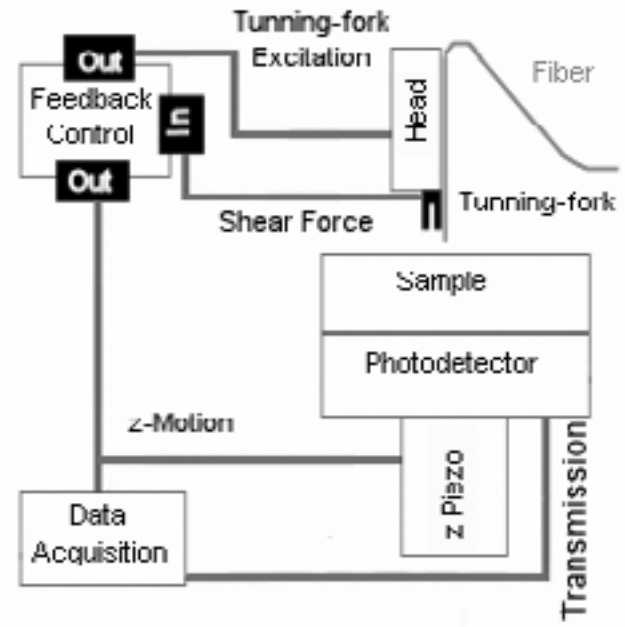

Fig.1- SNOM scheme working at constant gap mode. The shear force feedback and the probe fibre tip are the main differences with respect to a fully commercial AFM. The sample is illuminated through the fible tip under near field conditions, whereas the transmitted light is collected under far field by a germanium photodetector.

3. RESULTS AND DISCUSSION

Since the orientation of the surface in the sample studied is (0 0 1), the domain walls are expected to describe angles higher than 90º and close to 135º due to the fact that directions [1 1 0] and [-1 1 0] are expected to combine in this plane with [1 0 0] and [0 1 0]. In addition, [2 1 0] and [-2 1 0] directions could have been also observed. Figure 2 shows an optical microscope image of the sample after etching. Despite the low magnification (x100), two main regions can be easily distinguished: the left one, which is transparent to visible wavelengths, namely the C^+ domain; in the right side (top and bottom) the C^- domain can be observed. It is worth noting the metallic aspect of the C^- surface (when using polarized light to illuminate the sample), due to the surface roughness produced by the chemical attack. For this low magnification image the domain wall seems to be straight, which is not the case under higher magnifications.

AFM images enable us to quantify the effects of the chemical attack. Figure 3(a) shows the frontier between the two domains. We observe a rough surface for the C^- domain (left hand side of the image), as compare to the flat aspect

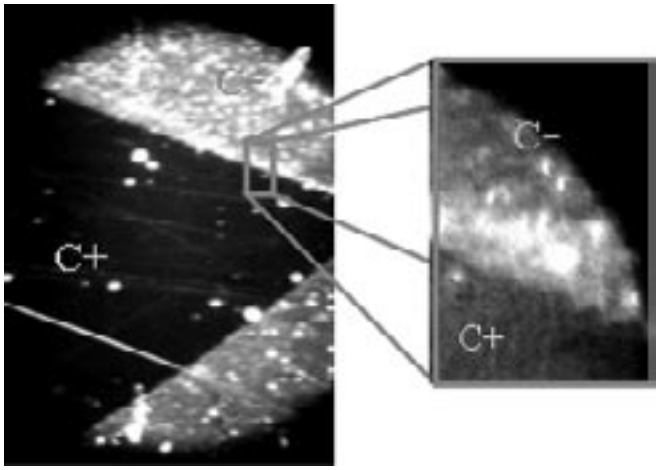

Fig.2- Photography obtained with an Optical Microscope of the RTP sample (x100 to x500 zoom). The transparent zone is the zone called C^+ (flat surface), while the ones that presents a metallic aspect are the C^- zones (rough surface). The small picture is a zoom of an area of the sample where the zig-zag chains, at the domain-wall, can be perfectly observed.

the domain wall in several places of it. In Figure 4(a) we show a typical SNOM topography image of the domain wall, obtained from an area of the sample close to that of the previous images studied with AFM. The two different roughness zones (i.e. the C^+ and C^- domains) can be also distinguished. A zoom extracted from the square in Figure 4(a) is shown in Figure 4(b). In Figs. 4(c) and 4(d) we show the profiles extracted from the green lines depicted in Figures 4(a) and 4(b), respectively. The step produced by the etching is clearly observed in Fig. 4(a), whose value is 40 nm [Fig. 4(c)] along the green line. The SNOM resolution can be estimated from Figure 4(d) to be around 6 nm along the normal direction to the surface, and better than 80-100 nm in the lateral directions.

The KTP family crystals tend to form straight domain walls oriented along the main directions at a macroscopic level (see x100 image in Figure 2). At a microscopic scale (x500 image in Figure 2) we do not observe those straight lines, but short segments with different orientations to that defined by the macroscopic straight line. This kind of phenomenology has been labelled as a zig-zag configuration (15). Our SNOM images are also consistent with this situation (see for example Figure 4). Note that this zig-zag shape (Fig, 2 and images

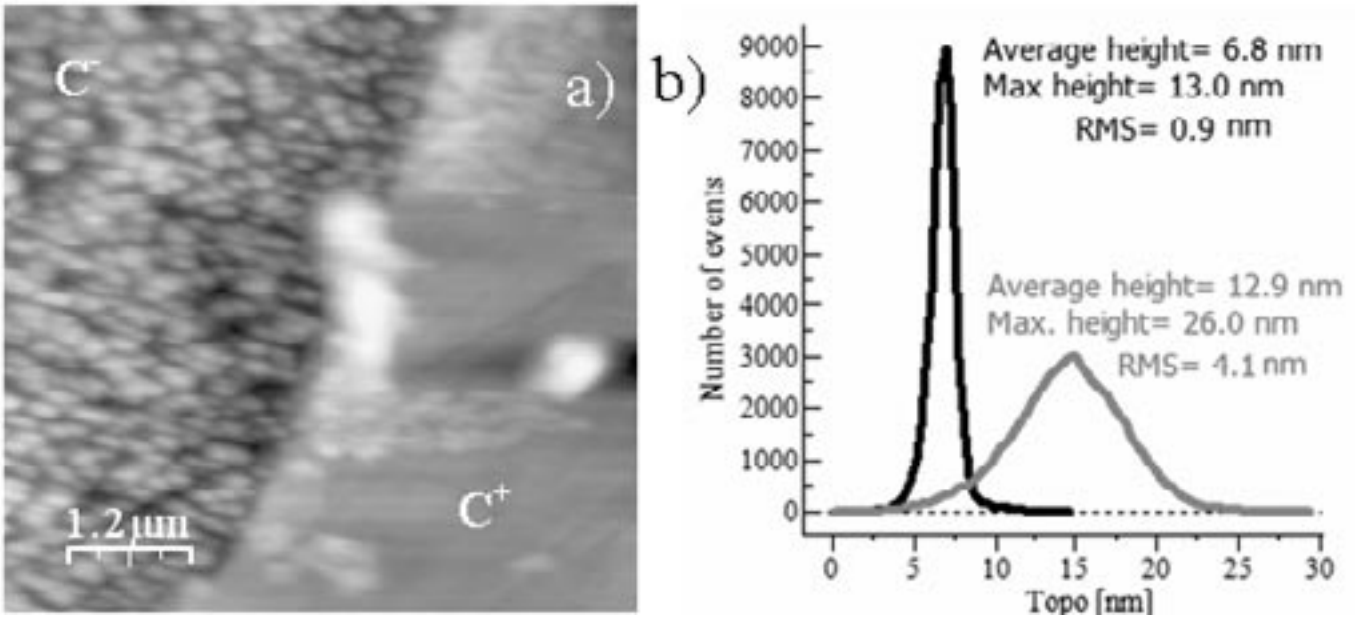

Fig.3- a) AFM image of the typical interface between both domains after etching (C^- zone, on the left and C^+ one on the right). b) AFM Roughness analysis of both images of each domain (not shown). The C^+ zone curve is represented in black, while the C^- one is in red (grey). The roughness differences are clearly observable in the height distribution and in the width of the fit.

of the C^+ domain (right side of the image). If we look at the image in more detail we also see other features that can be attributed to an inefficient etching zones or C^- nano-domains into the C^+ domain. AFM roughness measurements are quite sensitive to both the tip radius and the surface structure, so the roughness was compared for several images (not shown) in each domain far away of the domain walls, under the same scanning conditions. We have calculated the root mean square (RMS) roughness over all these images and plotted in Fig. 3(b). We find strong differences in the maximum relative height (6.8 and 13 nm for C^+ and C^-) and the RMS value (0.9 and 4.1 nm for C^+ and C^-).

We have recorded under similar conditions more than 100 images of topography plus transmission SNOM images along shown in Ref. 15) has been observed in an image obtained with an optical microscope und high resolution conditions. In most of our images, relative to small scanned areas of 10.5x10.5 μm^2, we have a lack of perspective and we typically observe a "straight portion" of the zig-zag wall. In a small number of cases we can clearly observe a zig-zag wall, now because the straight portions have sub-micrometric sizes. These effects are produced by the combination of the following main directions, [1 1 0] and [-1 1 0] with [1 0 0] and [0 -1 0]. We have measured the zig-zag angles along the entire domain wall. The result has been represented in Figure 5. We can confirm that straight segments define different angles, always higher than 90º and close to 135º (which is the most repeated value), the latter value being expected from the crystallographic point of view.

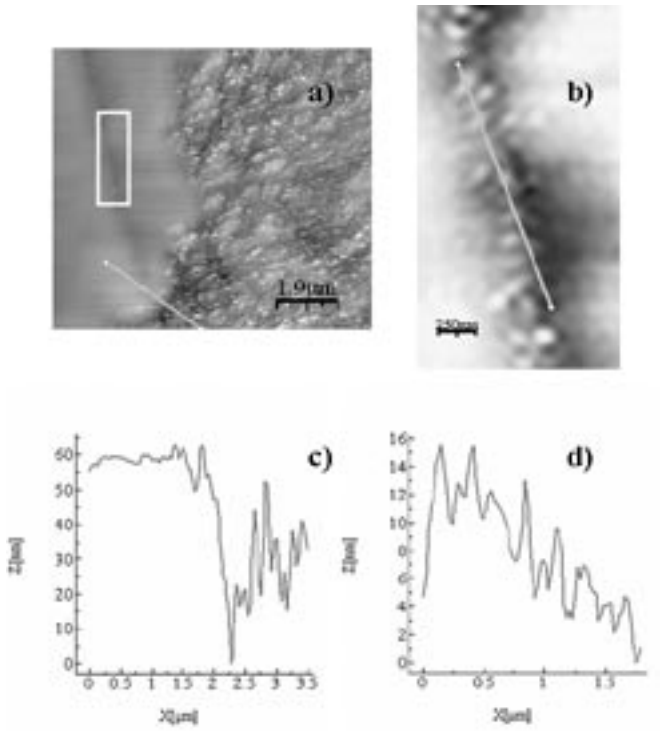

Fig.4- a) Typical interface (domain wall) with the C^- zone (rough surface) on the right and the C^+ one (flat surface) on the left. b) Zoom of the squared area in a). c) Profile extracted (from the image a)) above (marked with a line) showing the domain-wall step of around 40 nm. The topographic resolution of our SNOM is considered by analyzing a profile from b) (see figure d)) where details of less than 6 nm height and less than 80 nm width.

Finally, we have compared the SNOM transmission images obtained at different excitation wavelengths in a typical domain-wall zone of the sample. The results from these measurements, as well as the topography image, are shown in Figure 6. Both C^+ and C^- domain zones are also clearly distinguished, as well as the domain wall step, of around 30 nm high [Fig. 6(a)]. We observe in Fig. 6 how the domain wall

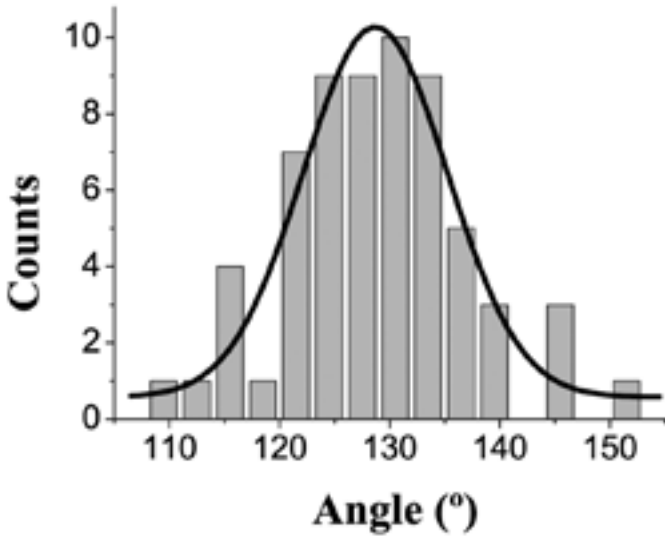

Fig.5- Interface angles distribution in intervals of 3º. The Gaussian fit is drawn with a continuous line.

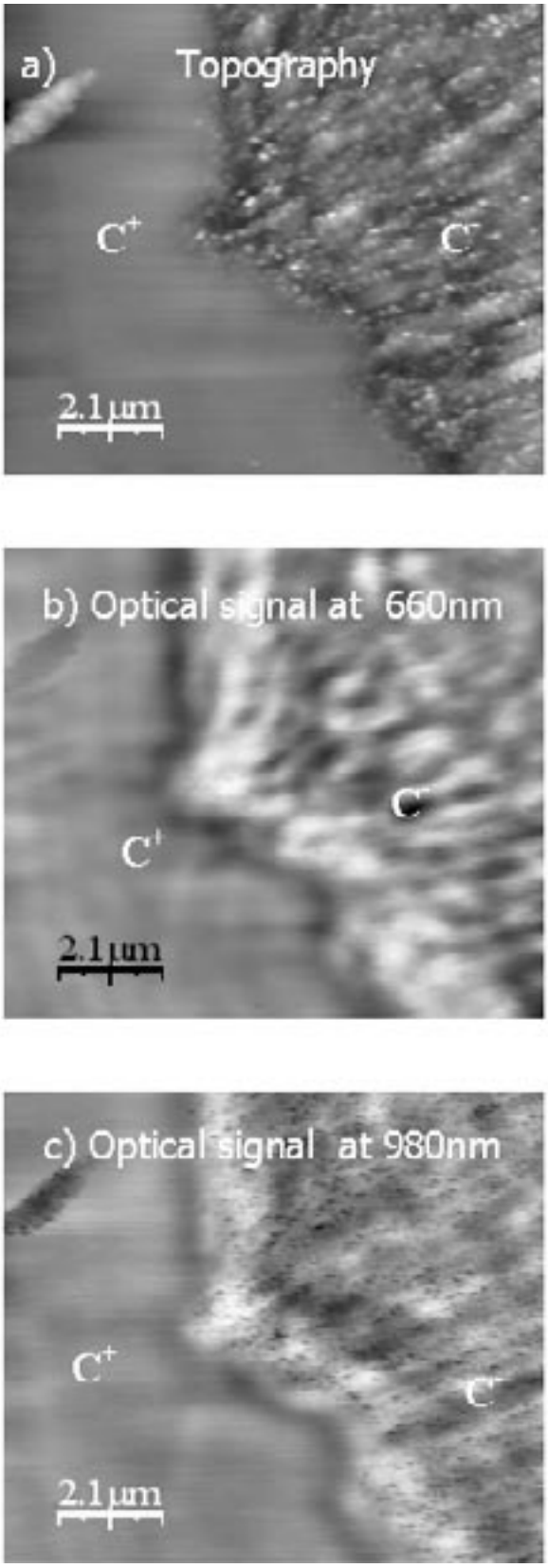

Fig.6- Boundary between the two ferroelectric domains present in the sample. a) SNOM topography. b) and c) transmission SNOM images obtained at 660 nm and 980 nm excitation wavelengths, respectively. Notice that the resolution is better with 980 nm.

step, as well as other topographic objects, are reproduced in the optical images with different contrast depending on the wavelength. From a topographic point of view, only the step produced by the chemical etching is clearly observed in the transmission image recorded at 660 nm [Fig. 6(b)], whereas most of the roughness features are also reproduced in the image recorded at 980 nm [Fig. 6(c)]. In addition to these topographic features we can observe some optical contrasts that cannot be associated to topographic objects and depend on the wavelength. It is worth noting the greater transmittance along the domain wall, within a region whose width is around 2 microns [Figs. 6(b) and (c)]. The step height between domains was approximately 30 nm, giving an optical contrast of 150 mV in the image recorded at 980 nm. This optical contrast seems too large to be only due to pure topographical effect. We can also expect a certain contribution associated to the change of the refractive index at the domain walls (18). In Fig. 6 we find further evidences of this contribution: some topographic objects, different than the domain wall step, of around 70 nm high produces an optical contrast of only 70 mV (in the 980 nm image). This means that a double size object produces an optical contrast similar than that from the domain wall step. Therefore, the changes produced in the transmission SNOM at the domain walls is due (almost fifty / fifty) to the topographic step produced by the etching process and the dielectric constant variation at the interface between domains and its vicinity (18). Additionally, we also observe a strong contrast modulation in the C^+ domain, which now is more evident in the image recorded at 660 nm. We attribute such contrast modulation to be due to light scattering at the surface grains produced by the chemical attack. In fact, this modulation is less important in the 980 nm image, as expected for ligth scattering by grains smaller than the light wavelength.

Finally, we point out the importance of the SNOM technique in the characterization of the optical properties at the domain walls, without needing a selective etching. This has been demonstrated in a recent paper, where we have done similar experiments in a polished sample with a flat surface that presents quasi-periodic domain structures in a natural way throughout the sample surface (19).

4. CONCLUSIONS

We have acquired the SNOM transmission as well as the topography of an $RbTiOPO_4$ single crystal sample, with two different macroscopic ferroelectric domains. We have quantified the effect of the chemical etching performed in the sample surface to distinguish the domains with AFM measurements resulting in a 100 nm domain-wall step and two different roughness zones, corresponding to the domains. From the SNOM topography images, we have determined a lateral resolution better than 80 nm while we can resolve height changes up to 1 nm in the perpendicular direction to the surface. We have determined the angles formed at the domain-walls between C^+ and C^-, which resulted to be higher than 90º and close to 135º, as expected, from a crystallographic point of view. The domain wall follows right lines according to the crystallographic predictions, forming zigzag lines at nanometer scale. From the SNOM optical images, contrast changes produced in the transmission measurements are associated to different effects, like the dielectric constant variations at the interface between domains and the light scattering at the grains in the C^+ domain. The SNOM provides the possibility of characterizing optically ferroelectric domain walls at a microscopic scale, without the need of a selective etching and thus without damaging the sample, in the case where domain walls could be easily identified, like in periodic (periods in the 5-10 μm range).

ACKNOWLEDGEMENTS

We want to acknowledge the "Ministerio de Educación y Ciencia" of Spain for the financial support under the project MAT2002-4603-C05-02. L. Martín-Carrón wants also to acknowledge the "Ministerio de Educación y Ciencia" of Spain for the financial support under the contract "Juan de la Cierva".

REFERENCES

1. M.A. Paeleser and P.J. Moyer. "Near-field optics. Theory, instrumentation, and applications". John Wiley& sons, inc. (1996)
2. G. Binnig and C.F. Quate. "Atomic Force Microscope". Phys. Rev. Lett.56, 930-933 (1986)
3. Y.Martin, C.C.Williams, and H.K. Wickramaisinghe. "Atomic force microscope-force mapping and profiling on a sub 100-A scale". J. Appl. Phys. 61,4723-4729,(1987)
4. S. Belaidi, P. Girard, and G. Leveque. "Electrostatic forces acting on the tip in atomic force microscopy: Modelization and comparison with analytic expressions". J. Appl. Phys. 81, 1023-1030 (1996).
5. M. A. Lantz, S. J. O'Shea, and M. E. Welland. "Simultaneous force and conduction measurements in atomic force microscopy". Phys. Rev. B. 56, 15345-15352 (1997).
6. T.E Shäfer, M. Radmacher and R. Proksch. "Magnetic force gradient mapping". J. Appl. Phys. 94, 6525-6532 (2003).
7. S. Kawata, M. Ohtsu and M. Irie. "Nano-Optics". Springer-Verlag Berlin Heidelberg (2002).
8. M.E.Hagerman and K.R.Poeppelmeier. "Review of the structure and processing-defect-property relationships of potassium titanyl phosphate: a strategy for novel thin-film photonic devices". Chem. Mater. 7, 602-621 (1995).
9. P.A. Thomas, S.C. Mayo and B.E. Watts "Crystal Structures of $RbTiOAsO_4$, $KTiO(P_{0.58}As_{0.42})O_4$, $RbTiOPO_4$ and $(Rb_{0.465}K_{0.535})TiOPO4$, and Analysis of Pseudosymmetry in Crystals of the $KTiOPO_4$ Family". Acta Crvst. B48, 401-407 (1992).
10. M.N.Satyanarayan, A. Deepthy and H.L.Bhat. "Potassium titanyl Phosphate and its isomorphs: growth, properties and applications". Crit. Rev. Solid State. 24, 103-191 (1999).
11. J.J Carvajal, J.L. García-Muñoz, R. Solé, Jna. Gavaldà, J. Massons, X. Solans, F. Díaz and M. Aguilló. "Charge Self-compensation in the Nonlinear Optical crystals $Rb_{0.855}Ti_{0.955}Nb_{0.045}OPO_4$ and $RbTi_{0.927}Nb_{0.056}Er_{0.017}OPO_4$". Chem. Mater. 15, 2338-2345 (2003).
12. J.J Carvajal, R. Solé, J. Massons, X. Solans, M. Aguilló and F. Díaz. "A new self-doubling material: $RbTiOPO_4$(Nb, Ln)". Opt. Mater. 24, 425-430 (2003).
13. J.A. Armstrong and N. Bloembergen. "Interactions between Light Waves in a Nonlinear Dielectric" Phys. Rev. 127, 1918-1939 (1962).
14. S.D. Cheng, Y.Y. Zhu, Y.L. Lu and N.B. Ming. "Growth and transducer properties of an acoustic superlattice with its periods varying gradually". Appl. Phys. Lett. 66, 291-292 (1995).
15. Z.W. Hu, P.A. Thomas and P.Q. Huang. "High-resolution x-ray diffraction and topographic study of ferroelectric domains and absolute structural polarity of $KTiOPO_4$ via anomalous scattering". Physical Review B. 56, 8559-8565 (1997).
16. F. Laurell, M.G Roelofs, W. Bindloss, H. Hsiung, A. Suna, and J.D. Bierlein. "Detection of ferroelectric domain reversal in $KTiOPO_4$ waveguides". J. Appl. Phys. 71, 4664-4670 (1992).
17. C. Zaldo, M. Rico, F. Diaz, J.J. Carvjal. "Crystal Growth of $RbTiOPO_4$: Nb: a new nonlinear optical host for rare earth doping". OPt Mater 13, 175-150 (1999).
18. H. Chaib, T. Otto and L.M. Eng. "Theorical study of ferroelectric and optical properties in the 180º ferroelectric domain wall of tetragonal $BaTiO_3$". Phys. Stat. Sol. (b). 233, 250-262 (2002).
19. J. Canet-Ferrer, L. Martín-Carrón, J. L. Valdés, J. Martínez-Pastor and C. Zaldo "Scanning Probe Microscopy Applied To The Study Of Domains And Domain Walls In A Ferroelectric $KNbO_3$ Crystal". Bol. Soc. Esp. Ceram.V. 45, 3, 218-222 (2006).

Recibido: 15.07.05
Aceptado: 10.03.06